Electronic structure α'-NaV_2O_5: Wave-function-based embedded-cluster calculations

L. Hozoi,[1] C. Presura,[2] C. de Graaf,[3] and R. Broer[1]

[1]*Theoretical Chemistry, Materials Science Centre, Rijksuniversiteit Groningen, Nijenborgh 4, Groningen 9747 AG, The Netherlands*

[2]*Department of Solid State Physics, Materials Science Centre, Rijksuniversiteit Groningen, Nijenborgh 4, Groningen 9747 AG, The Netherlands*

[3]*Department of Physical and Inorganic Chemistry, Universitat Rovira i Virgili, Plaça Imperial Tàrraco 1, Tarragona 43005, Spain*

(Received 12 September 2002; published 30 January 2003)

Results of *ab initio* embedded-cluster calculations indicate that the doublet ground state of the V-O_R-V rung originates from a V $3d^1_{xy}$–$O_R 2p^1_y$–V $3d^1_{xy}$ configuration. In the high temperature undistorted geometry the unpaired electron on oxygen is low-spin coupled to the $3d$ electrons and spin density is equally distributed over the vanadium ions. Based on this picture of the electronic ground state we propose a mechanism for the phase transition at 34 K. We find that a symmetry-broken configuration, $R(V_i\text{-}O_R) < R(V_j\text{-}O_R)$, leads to $V_i 3d_{xy}$–$O_R 2p_y$ spin singlet formation and stronger V_i-O_R bonding. We suggest that the onset of the phase transition at 34 K is driven by the shift of the bridging rung oxygen towards one of the V neighbors. The calculations predict a reduction of the exchange coupling constant of about 25% when distorting the V-O_R-V rung. At the same time, structural distortions involving the O_L leg oxygens induce alternation of the coupling constant and therewith spin-gap behavior.

DOI: 10.1103/PhysRevB.67.035117 PACS number(s): 71.70.−d, 75.50.Ee, 78.20.Bh

I. INTRODUCTION

The coupling of charge, spin, orbital, and lattice degrees of freedom is essential in understanding the physics of several classes of transition-metal materials. Typical examples are the perovskite manganese oxides, where such an interplay is responsible for the complex phase diagrams and unusual physical properties. For NaV_2O_5 it is presently believed that correlation of the charge, spin, and lattice degrees of freedom is involved in the phase transition at about 34 K.[1] Analysis of the specific-heat anomaly at $T_c \approx 34$ K (Refs. 2–6) shows indeed that a large part of the associated entropy, at least 75% according to Ref. 6, must be due to crystallographic distortions and/or charge redistribution within the vanadium-oxygen layers. A smaller fraction, probably less than 25%,[6] is connected to the magnetic subsystem. The temperature dependence of the dielectric function also displays an anomalous behavior[7,8] and confirms that at low temperatures (LT) charge redistribution occurs.

Crystallographically NaV_2O_5 consists of quasi-two-dimensional layers of VO_5 square pyramids, separated by Na ions. Within these layers the vanadiums are arranged in a network of two-leg ladders. The basic unit of the electronic structure of this material is formed by the V-O-V rung. Early x-ray-diffraction (XRD) measurements reported a noncentrosymmetric geometry with $V^{4+}3d^1$–$V^{5+}3d^0$ charge separation on the rungs of the ladder.[9] However, later XRD (Refs. 10 and 11) and nuclear magnetic resonance (NMR) (Ref. 12) experiments showed that at room temperature all V ions are equivalent, presumably in a $V^{4.5+}$ average valence state. Based on density-functional band-structure calculations[11] and model Hamiltonian studies,[11,13] NaV_2O_5 was associated to a quarter filled insulating ladder system. In this interpretation the d electron is not attached to a single V ion, but to a V $3d_{xy}$–V $3d_{xy}$ bonding molecular orbital, where the x and y directions are, respectively, along the a and b axes of the $Pmmn$ reference system. The V-V rung molecular clusters are antiferromagnetically coupled along the legs of the ladder and form parallel quasi-one-dimensional $S=1/2$ Heisenberg chains. Such a spin model explains the behavior of the magnetic susceptibility at temperatures above 200 K.[5,6]

NMR (Refs. 12 and 14) and XRD (Refs. 15–18) measurements show that at least two inequivalent vanadium sites exist below 34 K. This inequivalency was associated to a $2\,V^{4.5+} \rightarrow V^{4.5-\delta_c} + V^{4.5+\delta_c}$ charge ordering process. Several charge ordered models have been proposed for the LT phase, based on either in-line[19] or zigzag[20–22] charge ordering. Recent experimental results, i.e., the temperature dependence of the dielectric function,[7,8] the anomalous x-ray scattering at the vanadium K-edge,[23,24] and the sound velocity data,[25] seem to support a zigzag pattern as considered in Refs. 20–22. The authors of Refs. 18 and 24 also predict competing stacking arrangements along the c axis, perpendicular to the vanadium-oxygen layers.

A more recent interpretation of the electronic structure of NaV_2O_5 was derived from results of *ab initio* quantum chemical embedded-cluster calculations.[26] The analysis of Ref. 26 indicates that the doublet ground state (GS) of the V-O-V rung has actually predominant V $3d^1_{xy}$–O $2p^1_y$–V $3d^1_{xy}$ character. The high temperature (HT) magnetic structure can still be described by a spin model similar to that proposed by Horsch and Mack,[13] with an effective $S=1/2$ spin on each rung and antiferromagnetic (AFM) coupling along the ladder. In this paper we extend the analysis of Ref. 26 to the LT phase. We also propose a mechanism for the phase transition at 34 K. We argue that the charge redistribution which occurs in the ab plane at the transition point is connected mainly to a zigzag ordering of the V ions and of the oxygens on the rung, O_R, and not to $V^{4.5-\delta_c}$–$V^{4.5+\delta_c}$ electron localization.

II. COMPUTATIONAL INFORMATION

To determine the character of the GS and of the lowest excitations below and above T_c we have carried out elec-

tronic structure calculations on $[V_2O_9]^{9-}$ clusters including two VO_5 pyramids on the same rung. Our analysis is based on the complete active space self-consistent field (CASSCF) method,[27] as implemented in the MOLCAS 5 package.[28] The CASSCF approach involves a partitioning of the occupied orbitals into two sets: inactive orbitals that are doubly occupied, and active orbitals with occupation numbers between 0 and 2. The cluster wave functions are obtained as linear combinations of all the configurations that can be constructed by distributing the active electrons, i.e., those that are not in the doubly occupied inactive orbital set, among the active orbitals. In NaV_2O_5 strong interactions across the V-O_R-V rung occur through $3d_{xy}$-$2p_y$-$3d_{xy}$ π overlap. A minimal CAS should consist then of three active orbitals, the two V $3d_{xy}$ plus the bridging $O_R 2p_y$, and three active electrons. Here we present results of such minimal CAS calculations. To characterize and clarify the nature of the phase transition several geometric configurations have been considered. These are the $Pmmn$ HT crystal structure as determined by Meetsma *et al.*,[10] the $Fmm2$ LT configuration proposed by Bernert *et al.*,[16] and the $A112$ lattice system reported by Sawa *et al.*[17]

Adjacent rungs on the same ladder are antiferromagnetically coupled. In Ref. 26 we estimated the HT exchange coupling constant along the b axis by applying a second-order perturbational treatment to the CASSCF reference wave functions. This method is referred to as CASPT2.[29] Due to so-called intruder states we used there the level shift technique proposed by Roos and Anderson.[30] Since for different level shifts slightly different values are obtained for the coupling constant, some degree of uncertainty was contained in the results. However, rather good agreement was found with the experimental estimates from Refs. 1,5 and 6. In this paper we analyze the spin-gap formation in the LT phase. It has been suggested that the spin-gap originates from an alternation of the exchange constant $J_1 - J_2$ along the quasi-one-dimensional spin chain,[21] due to alternation of the V-O_L-V angles along the b axis,[16] where O_L is the bridging oxygen on the leg of the ladder. An unambiguous evaluation of the alternation parameter is difficult by CASPT2, because for adjacent V_4 plaquettes, J_1 and J_2 reach converged CASPT2 values when using different level shifts. To avoid intruder state problems and the use of level shifts we therefore resort to a variational approach, namely the difference dedicated configuration interaction (DDCI) method.[31,32] The states defining J, i.e., the singlet and the triplet corresponding to low- and high-spin coupling of the $S=1/2$ effective spins on each rung, are expressed in terms of CI expansions including single and double excitations from the CAS reference wave functions. It has been shown[31,33] that up to second order double excitations from the inactive space to the virtual orbitals equally contribute to the energy eigenvalues of the singlet and triplet states. Using the labels from Ref. 31, $p, q, \ldots$ for the inactive orbitals, $a, b, \ldots$ for the active orbitals, and $i, j, \ldots$ for the virtuals, such excitations are denoted as $pq \rightarrow ij$. By excluding these doubly excited determinants from the CI list, the size of the problem is reduced considerably. This computational scheme predicts spin coupling parameters in excellent agreement with experimental data and has been successfully applied for the study of magnetic interactions in several ionic insulators.[34,35] DDCI calculations are computationally too expensive in NaV_2O_5, since the $[V_4O_{16}]^{14-}$ cluster needed to extract the coupling between spins on adjacent rungs is relatively large, and the reference active space consists of no less than six orbitals (four V $3d_{xy}$ and two $O_R 2p_y$) and six electrons. For this reason we employ the so-called DDCI2 scheme,[31,34] where $pa \rightarrow ij$ and $pq \rightarrow cj$ excitations are excluded also from the CI expansion. DDCI2 usually yields 50–80 % of the experimental coupling constant.[35] We show below that even at this level valuable information can be obtained about the LT spin-gapped phase.

As described in previous work,[26] we represent the long-range crystalline environment by a set of point charges which reproduces the Madelung potential in the cluster region. The nearest vanadium and sodium neighbors are modeled by total ion potentials.[36] The cluster orbitals are constructed as linear combinations of atomic natural orbital (ANO) Gaussian-type functions. We applied the following basis sets:[37] V $(21s15p10d6f)/(6s5p4d1f)$ for vanadium and O $(14s9p4d)/(4s3p1d)$ for oxygen in the $[V_2O_9]^{9-}$ bi-pyramidal clusters; V $(21s15p10d)/(5s4p3d)$ for vanadium, O $(14s9p4d)/(4s3p1d)$ for O_L, O $(14s9p)/(4s3p)$ for O_R, and O $(14s9p)/(3s2p)$ for the other oxygens, in the larger $[V_4O_{16}]^{14-}$ clusters, including two adjacent rungs on the same ladder. The DDCI2 calculations have been performed with the CASDI code.[38]

III. RESULTS AND DISCUSSION

A. The electronic ground state

Table I lists CASSCF results for the ground and first two excited states of a $[V_2O_9]$ bi-pyramidal rung cluster. We report relative energies, charge Mulliken populations (MP's), and spin MP's of the V d_{xy} and $O_R p_y$ atomic basis functions, in three different geometries. In the HT $Pmmn$ crystal structure,[10] the point-group symmetry of the $[V_2O_9]$ cluster is C_{2v}. The GS and the lowest excited doublet, which defines the optical gap, transform according to the A_2 and B_2 irreducible representations, respectively, and can be denoted as $^2A_2$ and $^2B_2$. HT CASSCF results, discussed previously in Ref. 26, are given in the first column of Table I. According to XRD crystal structure determinations, the symmetry of the rung cluster is lowered below T_c, either to C_s,[15,16] or to C_1[17] (the actual LT crystal structure still is a source of controversy). Results obtained in such low-symmetry geometric configurations are shown in the second and the third columns. In the second column structural data from Ref. 16 was used, where a $Fmm2$ lattice system with alternating modulated and nonmodulated ladders is considered. In this model, on adjacent ladders, the O_R oxygens are either at equal distances from the V ions of the same rung, or shifted towards one of them. We analyze here only the rung with unequal V-O_R distances. For simplicity we use for each set of calculations notations corresponding to C_{2v} symmetry, even if the actual symmetry is lower.

The clearest picture is acquired for the quartet $^4A_2$: there are three unpaired electrons, one $O_R 2p_y$ and two V $3d_{xy}$,

TABLE I. Relative energies, charge MP's, and spin MP's for the $^2A_2$ GS and the lowest two excited states, $^2B_2$ and $^4A_2$, in high- and low-temperature geometric configurations. CASSCF results for a $[V_2O_9]$ cluster with three electrons and three orbitals in the active space. The spin MP's are for maximum M_s.

Crystal structure	*Pmmn*	*Fmm*2	*A*112
Rel. en. (eV):			
$^2A_2$ (GS)	0	0	0
$^2B_2$	0.69	0.84	0.75
$^4A_2$	0.99	1.08	0.99
$^2A_2$-MP's: [a]			
$V_{Right}d_{xy}$	0.9, 0.6	0.9, 0.8 [b]	0.9, 0.8 [b]
$V_{Left}d_{xy}$	0.9, 0.6	0.8, 0.3	0.9, 0.3
O_Rp_y	1.0,-0.3	1.0,-0.2	1.0,-0.2
$^2B_2$-MP's: [a]			
$V_{Right}d_{xy}$	0.9, 0.0	0.9, 0.1	0.9, 0.0
$V_{Left}d_{xy}$	0.9, 0.0	0.9, 0.1	0.9, 0.1
O_Rp_y	0.9, 1.0	0.9, 0.9	0.9, 0.9
$^4A_2$-MP's: [a]			
$V_{Right}d_{xy}$	0.9, 0.9	0.9, 0.9	0.9, 0.9
$V_{Left}d_{xy}$	0.9, 0.9	0.9, 0.9	0.9, 0.9
O_Rp_y	0.9, 1.0	0.9, 1.0	0.9, 1.0

[a]For each atomic orbital, the first number is the charge MP, and the second is the spin MP.

[b]V_{Left}-O_R<V_{Right}-O_R.

coupled to maximum spin. We list the V d_{xy} and O_Rp_y charge and spin populations of this state for comparison with those of the doublets. This comparison clearly indicates that also the GS and the lowest excited doublet arise from the same V $3d^1_{xy}$–O_R $2p^1_y$–V $3d^1_{xy}$ electronic configuration.

As illustrated in Table I, the low-energy electronic states have $O_R2p^1_y$ character in all geometries. The major difference between the HT structure and the distorted configurations concerns the GS spin coupling scheme. Above T_c $^2A_2$ corresponds to a state where the *d* electrons are coupled to a triplet, and the spin on the bridging oxygen is doublet coupled to it. The spin density is equally distributed over the two vanadiums. In the low temperature crystal structures the V-O_R distances are unequal. In Table I we chose V_{Left}-O_R <V_{Right}-O_R. As a consequence, the O_R $2p_y$ electron and the nearest V $3d_{xy}$ couple to a singlet, and spin density is localized on the distant vanadium ion.

Transitions from the ground state to the $^2B_2$ state may be induced by *x*-polarized light. We assign the $^2B_2$ doublet to the peak observed at 0.9 eV in the *x*-polarized optical absorption.[39,40] This state implies a low-spin coupling of the two *d* electrons, resulting in spin density localized on the O_R oxygen. CASSCF calculations with three electrons and three orbitals in the active space predict a $^2A_2$-$^2B_2$ splitting of about 0.7 eV in the HT crystal structure. The authors of Ref. 41 pointed out that the position of the 0.9-eV peak hardly depends on the temperature, with a blue shift of approximately 0.03 eV from 300 to 4 K. This suggests that the change in the valence state of the V ions at the phase transition is very small. Our estimates for the LT $^2A_2$-$^2B_2$ splitting are in reasonable agreement with these experimental findings. Thus the first absorption peak shifts to higher energy by 0.15 eV in the geometric configuration reported by Bernert *et al.*,[16] and 0.06 eV in the configuration of Sawa *et al.*[17] The GS total Mulliken charges of the V_{Right} and V_{Left} centers differ by about $0.02e$ in the *Fmm*2 crystal structure and by less than $0.01e$ in *A*112. By performing DDCI2 calculations with a CAS reference including the two V $3d_{xy}$ orbitals and the O_R2p_y, Suaud and Lepetit[42] found in the *Fmm*2 structure a charge disproportionation of $0.045e$.

The results in Table I were obtained by using for each set of calculations identical embedding charges: $+3.0e$ for the V ions, $-1.0e$ for the rung and apex oxygens, O_R and O_A, $-2.0e$ for the other ligands, and $+1.0e$ for Na.[26] We mention, however, that the character and ordering of the lowest states are unchanged when a so-called zigzag charge ordered structure, with zigzag V-V charge disproportionation, is used for the embedding array.

States arising from configurations with a doubly occupied O_R2p_y orbital are calculated at 5.5–6.5 eV. Our calculations overestimate their relative energy, due to the partial neglect of dynamical electron correlation and of electronic relaxation effects in the crystal as response to the V $3d_{xy}\rightarrow O_R2p_y$ charge-transfer process.[26] The $O_R2p_y^2$ states can be represented as $^2B_2$ ($p^2d^1_-$) and $^2A_2$ ($p^2d^1_+$), where d_- and d_+ are essentially the symmetric and antisymmetric combinations of the two V $3d_{xy}$ orbitals and transform according to the B_2 and A_2 irreducible representations, respectively, whereas *p* has mostly O_R2p_y character and belongs to B_2. When distorting the $[V_2O_9]$ cluster, d_- and d_+ become right- and left-oriented linear combinations. $^2B_2$ ($p^2d^1_-$) can explain the nature of the peak at 3.3 eV of the *x*-polarized absorption spectrum.[26] We also assign the features above 3.5 eV in both *x* and *y* polarizations to $O_A2p\rightarrow$V $3d$ charge-transfer excitations. We note, however, that we cannot provide a simple explanation for the shoulder at 1.4 eV in the *x*-polarized spectrum and the *y*-polarized low-intensity excitations at 1–2 eV.

The present study evidences that both above and below T_c the doublet ground state of the V-O_R-V rung has oxygen $2p$-hole character. By distorting the rung, a spin singlet is formed on the side with the shortest V-O_R distance. Compared to the undistorted HT crystal structure, analysis of the cluster wave function indicates stronger $3d_{xy}$-$2p_y$ bonding for this V-O pair. In the following paragraphs we argue that the onset of the phase transition at 34 K is related to the formation of such a spin singlet when the bridging rung oxygen is shifted towards one of the V neighbors.

B. The phase transition

The XRD data[15–17,43] show that at low temperatures the major crystalline distortions take place along the *x* and *z* directions, and mainly involve displacements of the vanadium ions, the bridging O_R and the apex ligands. Projected

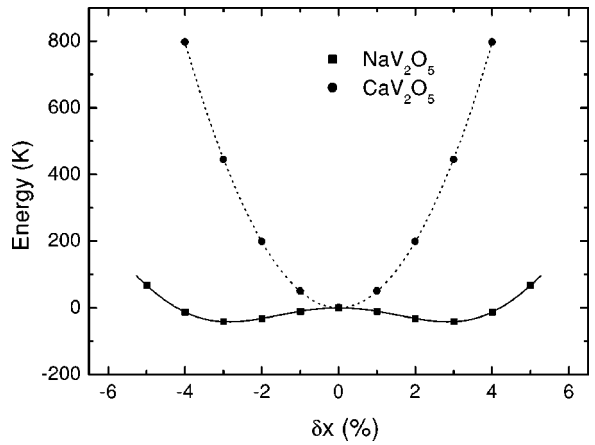

FIG. 1. The ground-state energy of a $[V_2O_9]$ cluster when the O_R oxygen is shifted along the V-V rung, in NaV_2O_5 and CaV_2O_5 (see text). The energy of the undistorted cluster is taken as reference.

on the x axis, the V_{Right}-O_R (V_{Left}-O_R) distance increases (decreases) by about 3%.[15–17] We analyze in this section the effect of shifting the rung oxygen along the x axis on the cluster GS energy. Starting from the HT crystal structure we gradually change the x coordinate of this ion relative to the adjacent V sites, by 1%, 2%, . . . , and 5%. We do not modify the positions of the other atoms in the $[V_2O_9]$ cluster, neither the embedding. The effect of such distortions is illustrated in Fig. 1. We take as reference the energy of the undistorted cluster. The double-well dependence is still obtained when the lattice parameters are modified within $\pm 5\%$.

Remarkably, the cluster GS energy displays a shallow double-well shape, reaching a minimum of 42 K for a distortion of 3%. These results suggest that a symmetry-broken configuration, with the bridging oxygen forming a stronger bond with one of the vanadium neighbors, could be energetically favored. For comparison we plot in Fig. 1 the same dependency, GS energy versus δx, for a $[V_2O_9]$ cluster in CaV_2O_5. This material is isostructural with the high temperature NaV_2O_5. The V-O distances in the VO_5 pyramids are very similar in the two compounds. However, the rung GS wave function has $V\,3d^1_{xy}$–$O_R 2p^6$–$V\,3d^1_{xy}$ character in CaV_2O_5. We used for this set of calculations the crystallographic data reported by Onoda and Nishiguchi.[44] In contrast to NaV_2O_5, the potential-energy curve displays a steep parabolic behavior, with a minimal value for $\delta x = 0$. We reiterate that the orbital occupation numbers and the ordering of the low-energy states are unchanged when distorting the V-O_R-V rung. For NaV_2O_5 we illustrate this in Table II.

The results in Fig. 1 are rather qualitative. A detailed analysis would require a preliminary geometry optimization, as well as a study of basis set effects. To explain the value of the transition temperature, the coupling between crystallographic distortions and lattice vibrations should be also taken into account. Nevertheless, the shape of the potential-energy curve in Fig. 1 strongly suggests that the phase transition is driven by such distortions of the rung oxygens. Moreover, in this scenario the O_R-O_R Coulomb repulsion should produce a

TABLE II. Relative energies, charge MP's, and spin MP's for the $^2A_2$ GS and the lowest excited doublet $^2B_2$ when the bridging rung oxygen is shifted along the x axis (see text). CASSCF results for a $[V_2O_9]$ cluster with three electrons and three orbitals in the active space. The spin MP's are for maximum M_s.

δx [a]	1%	3%	5%
Rel. en. (eV):			
$^2A_2$ (GS)	0	0	0
$^2B_2$	0.70	0.76	0.88
$^2A_2$-MP's: [b]			
$V_{Right}d_{xy}$	0.9, 0.7	0.9, 0.8	0.9, 0.8
$V_{Left}d_{xy}$	0.9, 0.5	0.9, 0.4	0.9, 0.3
$O_R p_y$	1.0,-0.3	1.0,-0.3	1.0,-0.2
$^2B_2$-MP's: [b]			
$V_{Right}d_{xy}$	0.9, 0.0	0.9, 0.0	0.9, 0.1
$V_{Left}d_{xy}$	0.9, 0.1	0.9, 0.1	0.9, 0.1
$O_R p_y$	0.9, 0.9	0.9, 0.9	0.9, 0.9

[a] V_{Left}-$O_R < V_{Right}$-O_R.
[b] For each atomic orbital, the first number is the charge MP, and the second is the spin MP.

zigzag arrangement of the rung oxygens on the same ladder. The other atoms in the crystal subsequently adjust to the new conformation, giving rise to the complex crystal structure observed at low temperatures.

An O_R-O_R zigzag conformation is consistent with the experimental findings of Smirnov *et al.*[7] and Poirier *et al.*[8] The dielectric anomalies observed near the transition point[7,8] show that below T_c an antiferroelectrically ordered structure is formed in the ab plane. The experimental data also indicate that the largest charge displacements occur along the a axis. To explain the antiferroelectric (AFE) ordering, the charge displacements should develop in opposite senses at neighboring sites. A zigzag arrangement of the rung oxygens fulfills these requirements. It has been actually determined that at low temperatures the O_R oxygens form indeed a zigzag, either on every second ladder,[15,16] or on all ladders.[17] In addition, according to Refs. 15–17, also the V ions are distributed in a zigzag manner, along each leg of these ladders. Since the two vanadiums and the O_R oxygen of the same rung are displaced along the a axis in opposite senses,[15–17] the AFE ordering in the ab plane can be naturally explained without invoking $V^{4.5-\delta_c}$–$V^{4.5+\delta_c}$ charge disproportionation.

C. Exchange interactions below T_c

CASSCF and iterative DDCI2 (IDDCI2) intraladder Heisenberg coupling constants are listed in Table III. It is well known that CASSCF calculations based on an active space that contains the magnetic orbitals correctly reproduce the sign of the magnetic interaction, but the magnitude of the coupling parameter is severely underestimated. The CASSCF accounts for the direct exchange plus the superexchange contribution of the Anderson model.[45] Effects that go beyond the CASSCF approximation, discussed by de Loth

TABLE III. Intraladder magnetic coupling constants in high- and low-temperature geometric configurations. CASSCF and IDDCI2 results for $[V_4O_{16}]$ clusters including two adjacent rungs. The reference CAS contains six electrons and six orbitals.

Crystal structure	*Pmmn*	*Fmm*2	*A*112
CASSCF :			
J_1 (K)	-90	-99	-69
J_2 (K)	-90	-82	-58
IDDCI2 :			
J_1 (K)	-398	-426	-299
J_2 (K)	-398	-376	-264
δ [a]		0.06	0.06

[a] $\delta=(J_1-J_2)/(J_1+J_2)$.

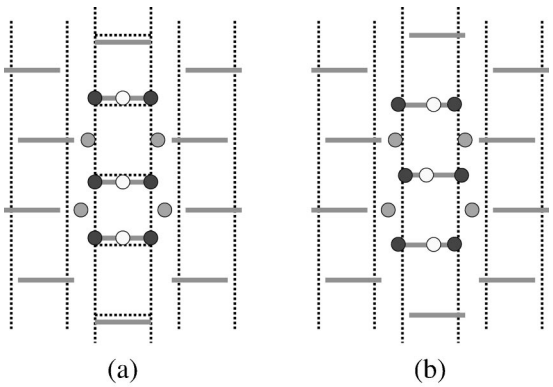

FIG. 2. Adjacent V_4 plaquettes on alternating-exchange ladders in the *Fmm*2 (a) and *A*112 (b) crystal structures. Black, grey, and white spheres represent vanadium, leg oxygen O_L, and rung oxygen O_R sites, respectively.

et al. in Ref. 46, can be incorporated by the DDCI technique.[31] In the DDCI scheme the results are dependent on the orbitals. In the iterative DDCI the orbitals are obtained in a self-consistent procedure.[32] The authors of Ref. 32 proposed to construct orbitals by diagonalizing the singlet-triplet average DDCI density matrix; with this orbital set, a new DDCI calculation is performed. The optimal orbitals for the property of interest are obtained by repeating the procedure until self-consistency.

For the *A*112 LT crystal structure[17] the calculated intraladder magnetic coupling constants are not equal on adjacent V_4 plaquettes (see the third column of Table III). This result supports the alternating-exchange chain model proposed by Mostovoy *et al.*[21] to explain the spin-gap formation at low temperatures. A major difference between the conclusions of Ref. 21 and our study is that we find no significant V-V charge disproportionation.

In the *Fmm*2 configuration,[15,16] alternation of the V-O_L-V angles and V-V distances in the *b* direction, and consequently alternation of the exchange coupling, occurs only on every second ladder (see Fig. 2). The results in the second column of Table III correspond to such an alternating-exchange ladder.[47] However, by symmetry, the spin moments on the remaining ladders should behave as an AFM uniform chain, which is inconsistent with the observed spin-gap. Even if a *Fmm*2 lattice system apparently cannot explain the spin-gapped state below 34 K, the *J* values given in the second column of Table III are illustrative for the effect of various crystallographic distortions on the strength of the magnetic coupling. In agreement with previous estimates,[16] our calculations indicate that the coupling parameter is more sensitive to the displacement of the bridging O_L oxygens along the *a* axis, than to the V-V dimerization along *b*. Thus, on adjacent V_4 plaquettes, the alternating coupling parameters of -426 and -376 K are mainly due to alternating O_L-O_L distances of 3.956 and 4.024 Å.

Within the alternating-exchange ladders of the *Fmm*2 system the O_R oxygens lie at the middle of the V-V rungs. In contrast, in the *A*112 structure each rung oxygen is shifted towards one of the two vanadiums. The results in Table III suggest that such a distortion leads to a significant decrease of the exchange coupling constant. To separate the effect of shifting the rung oxygens from the effect of other distortions, we performed additional calculations in a $[V_4O_{16}]$ cluster where, except the rung oxygens, all the other ions are at crystallographic positions corresponding to the room temperature structure. The two O_R ions are shifted along the *a* axis, as in the previous subsection, with $\delta x=\pm 3\%$. The resulting coupling parameter is about 25% smaller than the value in the high-symmetry cluster, -66 K by CASSCF and -306 K by IDDCI2. Compared with the alternating-exchange ladder of the *Fmm*2 crystal structure, the reduction of the average magnetic coupling constant, $J=(J_1+J_2)/2$, in the *A*112 system is approximately 30%.

As mentioned above, DDCI2 usually yields 50–80% of the experimental *J* (see Ref. 35 and references therein). Table III shows that IDDCI2 reproduces $\sim 70\%$ of the value deduced from magnetic susceptibility data for the HT phase, 560–580 K.[1,5,6] Although we cannot calculate coupling constants quantitatively, the data in Table III still allow us to predict the evolution of the intraladder exchange coupling around the phase transition. Thus we found that distorting the V-O_R-V rungs, the exchange coupling parameter decreases by 25–30 %. At the same time, structural distortions involving the O_L leg oxygens induce alternation of the exchange coupling parameter and therewith spin-gap behavior. We note that Gros and Valentí[48] explained the magnon dispersion observed in neutron-scattering measurements by assuming below T_c a reduction of the intraladder average exchange constant of 20–25 %. They also predict an exchange alternation parameter $\delta=(J_1-J_2)/(J_1+J_2)=0.034$, smaller than our estimates. Similar values for the alternation parameter, $\delta=0.028$–0.040, have been determined by Johnston *et al.*[6] from fits of the magnetic susceptibility. However, they assumed an effective exchange constant $J(T)$ which is either constant or increases with decreasing *T*, due to spin-phonon coupling.

IV. CONCLUSIONS

NaV_2O_5 was previously described either in terms of alternating $V^{4+}(3d^1)$ and $V^{5+}(3d^0)$ parallel chains[1,9] or as a

system of quarter filled V $3d^{0.5}$ ladders.[11] Both models assume a fully ionic picture of the material, with valence states of $2-$ for the oxygen ions. In contrast, *ab initio* quantum chemical calculations[26,49] indicate that the bridging oxygen on the rung of the ladder, O_R, and the apical ligand O_A should be considered as O^- ions, rather than O^{2-}. The calculations show also that states arising from a configuration with a hole in the $O_R 2p$ shell are the lowest in energy.[26]

We find that the ground state of the V-O_R-V rung has $3d^1_{xy}$–$2p^1_y$–$3d^1_{xy}$ character. In the high temperature undistorted geometry the unpaired electron on oxygen is low-spin coupled to the $3d$ electrons and spin density is equally distributed over the vanadium ions. A preliminary analysis of the effect of distorting the V $3d^1_{xy}$–$O_R 2p^1_y$–V $3d^1_{xy}$ rung on the ground state energy reveals that a symmetry-broken configuration, V_i-O_R<V_j-O_R, with $V_i 3d_{xy}$–O_R $2p_y$ spin singlet formation and stronger V_i-O_R bonding, can be energetically preferred. The energy gain calculated for this displacement is small, but relaxation of the other atoms in the crystal is expected to further stabilize the symmetry-broken configuration. We suggest that the energy gain upon the formation of the $V_i 3d_{xy}$–$O_R 2p_y$ spin singlet, when the bridging rung oxygen is shifted towards one of the adjacent V ions, determines the onset of the phase transition at 34 K. This model does involve charge redistribution, but not via significant V-V charge disproportionation.

Our results are able to explain the main features of the optical absorption and the AFM interaction along the *b* axis. We attribute the peak at 0.9 eV to a state characterized by a different spin coupling scheme among the valence V $3d_{xy}$ and $O_R 2p_y$ electrons; the features above 3 eV are assigned to V $3d \rightarrow O_R 2p$ and $O_A 2p \rightarrow$ V $3d$ charge-transfer excitations. We predict a reduction of the exchange coupling constant of about 25% when distorting the V-O_R-V rung. At the same time, structural distortions involving the O_L leg oxygens induce alternation of the coupling constant and therewith spin-gap behavior.

ACKNOWLEDGMENTS

This work was sponsored by the Netherlands National Computer Facilities Foundation (NCF). We thank G. Maris, J. Cabrero, R. Caballol, G. A. Sawatzky, M. V. Mostovoy, D. I. Khomskii, and J. W. Brill for help and stimulating discussions.

[1] M. Isobe and Y. Ueda, J. Phys. Soc. Jpn. **65**, 1178 (1996).
[2] M. Köppen, D. Pankert, R. Hauptmann, M. Lang, M. Weiden, C. Geibel, and F. Steglich, Phys. Rev. B **57**, 8466 (1998).
[3] D. K. Powell, J. W. Brill, Z. Zeng, and M. Greenblatt, Phys. Rev. B **58**, 2937 (1998); E. Postolache, D. K. Powell, G. Popov, R. C. Rai, M. Greenblatt, and J. W. Brill, Solid State Sci. **2**, 759 (2000).
[4] W. Schnelle, Yu. Grin, and R. K. Kremer, Phys. Rev. B **59**, 73 (1999).
[5] J. Hemberger, M. Lohmann, M. Nicklas, A. Loidl, M. Klemm, G. Obermeier, and S. Horn, Europhys. Lett. **42**, 661 (1998).
[6] D. C. Johnston, R. K. Kremer, M. Troyer, X. Wang, A. Klümper, S. L. Bud'ko, A. F. Panchula, and P. C. Canfield, Phys. Rev. B **61**, 9558 (2000).
[7] A. I. Smirnov, M. N. Popova, A. B. Sushkov, S. A. Golubchik, D. I. Khomskii, M. V. Mostovoy, A. N. Vasil'ev, M. Isobe, and Y. Ueda, Phys. Rev. B **59**, 14 546 (1999).
[8] M. Poirier, P. Fertey, J. Jegoudez, and A. Revcolevschi, Phys. Rev. B **60**, 7341 (1999).
[9] A. Carpy and J. Galy, Acta Crystallogr., Sect. B: Struct. Crystallogr. Cryst. Chem. **31**, 1481 (1975); A. Carpy, A. Casalot, M. Pouchard, J. Galy, and P. Hagenmuller, J. Solid State Chem. **5**, 229 (1972).
[10] A. Meetsma, J. L. de Boer, A. Damascelli, J. Jegoudez, A. Revcolevschi, and T. T. M. Palstra, Acta Crystallogr., Sect. C: Cryst. Struct. Commun. **54**, 1558 (1998); H. G. von Schnering, Yu. Grin, M. Kaupp, M. Somer, R. K. Kremer, O. Jepsen, T. Chatterji, and M. Weiden, Z. Kristallogr. **213**, 246 (1998); T. Chatterji, K. D. Liβ, G. J. McIntyre, M. Weiden, R. Hauptmann, and C. Geibel, Solid State Commun. **108**, 23 (1998).
[11] H. Smolinski, C. Gros, W. Weber, U. Peuchert, G. Roth, M. Weiden, and C. Geibel, Phys. Rev. Lett. **80**, 5164 (1998).
[12] T. Ohama, H. Yasuoka, M. Isobe, and Y. Ueda, Phys. Rev. B **59**, 3299 (1999).
[13] P. Horsch and F. Mack, Eur. Phys. J. B **5**, 367 (1998).
[14] Y. Fagot-Revurat, M. Mehring, and R. K. Kremer, Phys. Rev. Lett. **84**, 4176 (2000).
[15] J. Lüdecke, A. Jobst, S. van Smaalen, E. Morré, C. Geibel, and H.-G. Krane, Phys. Rev. Lett. **82**, 3633 (1999); J. L. de Boer, A. Meetsma, J. Baas, and T. T. M. Palstra, *ibid.* **84**, 3962 (2000).
[16] A. Bernert, T. Chatterji, P. Thalmeier, and P. Fulde, Eur. Phys. J. B **21**, 535 (2001).
[17] H. Sawa, E. Ninomiya, T. Ohama, H. Nakao, K. Ohwada, Y. Murakami, Y. Fujii, Y. Noda, M. Isobe, and Y. Ueda, cond-mat/0109164 (unpublished).
[18] S. van Smaalen, P. Daniels, L. Platinus, and R. K. Kremer, Phys. Rev. B **65**, 060101 (2002).
[19] P. Thalmeier and P. Fulde, Europhys. Lett. **44**, 242 (1998).
[20] H. Seo and H. Fukuyama, J. Phys. Soc. Jpn. **67**, 2602 (1998).
[21] M. V. Mostovoy and D. I. Khomskii, Solid State Commun. **113**, 159 (2000).
[22] M. V. Mostovoy, D. I. Khomskii, and J. Knoester, Phys. Rev. B **65**, 064412 (2002).
[23] H. Nakao, K. Ohwada, N. Takesue, Y. Fujii, M. Isobe, Y. Ueda, M. v. Zimmermann, J. P. Hill, D. Gibbs, J. C. Woicik, I. Koyama, and Y. Murakami, Phys. Rev. Lett. **85**, 4349 (2000); J. Garcia and M. Benfatto, *ibid.* **87**, 189701 (2001); J. E. Lorenzo, S. Bos, S. Grenier, H. Renevier, and S. Ravy, *ibid.* **87**, 189702 (2001).
[24] S. Grenier, A. Toader, J. E. Lorenzo, Y. Joly, B. Grenier, S. Ravy, L. P. Regnault, H. Renevier, J. Y. Henry, J. Jegoudez, and A. Revcolevschi, Phys. Rev. B **65**, 180101 (2002).

[25] H. Schwenk, S. Zherlitsyn, B. Lüthi, E. Morre, and C. Geibel, Phys. Rev. B **60**, 9194 (1999).
[26] L. Hozoi, A. H. de Vries, A. B. van Oosten, R. Broer, J. Cabrero, and C. de Graaf, Phys. Rev. Lett. **89**, 076407 (2002).
[27] B. O. Roos, P. R. Taylor, and P. E. M. Siegbahn, Chem. Phys. **48**, 157 (1980).
[28] MOLCAS 5, Department of Theoretical Chemistry, University of Lund, Sweden.
[29] K. Andersson, P.-Å. Malmqvist, B. O. Roos, A. J. Sadlej, and K. Wolinski, J. Phys. Chem. **94**, 5483 (1990); K. Andersson, P.-Å. Malmqvist, and B. O. Roos, J. Chem. Phys. **96**, 1218 (1992).
[30] B. O. Roos and K. Andersson, Chem. Phys. Lett. **245**, 215 (1995).
[31] J. Miralles, J.-P. Daudey, and R. Caballol, Chem. Phys. Lett. **198**, 555 (1992); J. Miralles, O. Castell, R. Caballol, and J.-P. Malrieu, Chem. Phys. **172**, 33 (1993).
[32] V. M. García, O. Castell, R. Caballol, and J. P. Malrieu, Chem. Phys. Lett. **238**, 222 (1995).
[33] J. P. Malrieu, J. Chem. Phys. **47**, 4555 (1967).
[34] I. de P. R. Moreira, F. Illas, C. J. Calzado, J. F. Sanz, J.-P. Malrieu, N. Ben Amor, and D. Maynau, Phys. Rev. B **59**, 6593 (1999).
[35] C. de Graaf, I. de P. R. Moreira, F. Illas, and R. L. Martin, Phys. Rev. B **60**, 3457 (1999); C. de Graaf and F. Illas, *ibid.* **63**, 014404 (2000); C. J. Calzado, J. F. Sanz, and J. P. Malrieu, J. Chem. Phys. **112**, 5158 (2000); D. Muñoz, F. Illas, and I. de P. R. Moreira, Phys. Rev. Lett. **84**, 1579 (2000).
[36] P. Durand and J. C. Barthelat, Theor. Chim. Acta **38**, 283 (1975).
[37] R. Pou-Amérigo, M. Merchán, I. Nebot-Gil, P.-O. Widmark, and B. O. Roos, Theor. Chim. Acta **92**, 149 (1995); P.-O. Widmark, P.-Å. Malmqvist, and B. O. Roos, *ibid.* **77**, 291 (1990).
[38] CASDI, Laboratoire de Physique Quantique, Université Paul Sabatier, Toulouse, France.
[39] S. A. Golubchik, M. Isobe, A. N. Ivlev, B. N. Mavrin, M. N. Popova, A. B. Sushkov, Y. Ueda, and A. N. Vasil'ev, J. Phys. Soc. Jpn. **66**, 4042 (1997).
[40] A. Damascelli, D. van der Marel, M. Grüninger, C. Presura, T. T. M. Palstra, J. Jegoudez, and A. Revcolevschi, Phys. Rev. Lett. **81**, 918 (1998); C. Presura, D. van der Marel, M. Dischner, C. Geibel, and R. K. Kremer, Phys. Rev. B **62**, 16 522 (2000).
[41] C. Presura, D. van der Marel, A. Damascelli, and R. K. Kremer, Phys. Rev. B **61**, 15 762 (2000).
[42] N. Suaud and M.-B. Lepetit, Phys. Rev. Lett. **88**, 056405 (2002).
[43] S. Ravy, J. Jegoudez, and A. Revcolevschi, Phys. Rev. B **59**, 681 (1999).
[44] M. Onoda and N. Nishiguchi, J. Solid State Chem. **127**, 359 (1996).
[45] P. W. Anderson, Phys. Rev. **115**, 2 (1959); R. K. Nesbet, *ibid.* **119**, 658 (1960).
[46] P. de Loth, P. Cassoux, J. P. Daudey, and J. P. Malrieu, J. Am. Chem. Soc. **103**, 4007 (1981).
[47] It is the ladder represented in Fig. 1 of Ref. 16 by V_{1b} vanadium sites. The V_{1a} and V_{1b} ladders are not equivalent.
[48] C. Gros and R. Valentí, Phys. Rev. Lett. **82**, 976 (1999).
[49] N. Suaud and M.-B. Lepetit, Phys. Rev. B **62**, 402 (2000).